Field Distributions in Six-port Gyroelectric Semiconductor Circulators with Coplanar Waveguide (CPW) Feeders

Zee M. Ng, Lionel E. Davis and Robin Sloan

Dept. of Electrical Engineering and Electronics, University of Manchester Institute of Science and Technology (UMIST), P.O. Box 88, Sackville Street, Manchester M60 1QD, U.K.

Abstract — **The magnetic field distributions of a CPW semiconductor junction circulator are computed at different frequencies for the first time. The results resemble the electric field distributions of a six-port microstrip ferrite junction circulator simulated using Ansoft HFSS. A broadband CPW semiconductor circulator centered at 60GHz has been designed by tracking the perfect circulation curves from the region where $\varepsilon_{eff}>0$ up to the region where $\varepsilon_{eff}<0$.**

I. INTRODUCTION

The integration of nonreciprocal ferrite components into Monolithic Microwave Integrated Circuits (MMICs) poses both materials and microwave signal problems. However, nonreciprocity can also be obtained with a gyrotropic semiconductor. A magnetized semiconductor gives rise to a permittivity tensor instead of the permeability tensor experienced in magnetized ferrites. The first semiconductor junction circulator operating at frequencies range 20-40 GHz at 77K, supported by three symmetrically positioned finlines feeders has been experimentally demonstrated in [1]. This demonstration has proven the fact that circulating effects can also be obtained in semiconductor circulators. However, a problem arises because finlines are not the common interconnects used in MMICs. Microstrip and coplanar lines are the two most common interconnects in MMICs. Since coplanar lines provide the correct electromagnetic field orientations for the excitation of the TE mode such that the electric field across the slot equates to the angular electric field in the semiconductor disc, it is therefore important to be able to design a semiconductor junction circulator having coplanar waveguide (CPW) feeders instead of finlines. In this paper, we present the magnetic field distributions of a CPW semiconductor junction circulator and show resemblance to the electric field distributions of a six-port microstrip ferrite junction circulator. By tracking the perfect circulation curves, we designed a broadband CPW semiconductor circulator centered at 60 GHz.

II. THEORETICAL BACKGROUND

A theoretical study on the CPW semiconductor junction circulator [2] has been presented by extending the existing three-port semiconductor junction circulator analysis. In this analysis, a CPW input with an odd mode excitation is represented as two slot feeds in which the signals are equal in magnitude but 180° out of phase. The six-slot circulator structure is similar to the Y-junction circulator discussed in [1-3]. Each of the slots subtends an angle of 2ψ with the center of the disc, where ψ is known as the coupling half-angle. Fig. 1 shows the six-slot circulator structure and the unusual location of slots has been justified in [2]. Slots 1 and 2, slots 3 and 4, and slots 5 and 6 are diametrically located, and each pair of slots forms one CPW input port such that the signals of each linked pair of slots are equal in magnitude but 180°out of phase.

The ideal boundary conditions on the semiconductor disc are similar to the three-port semiconductor disc, i.e. the electric wall exists on the curved surface except at the apertures of the ports and the air/semiconductor interfaces on the top and bottom of the thin disc form the magnetic wall.

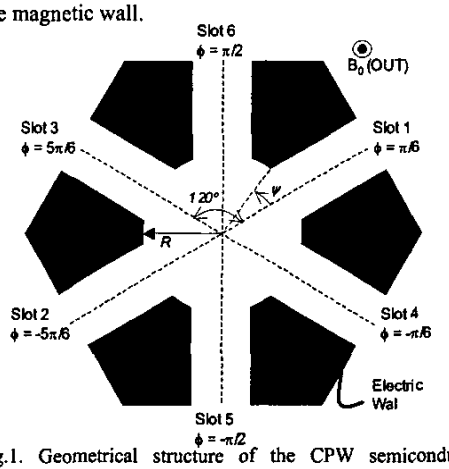

Fig.1. Geometrical structure of the CPW semiconductor junction circulator

III. GREEN'S FUNCTION

The general solution for the electromagnetic field distribution in the six-slot semiconductor disc involves Green's functions. Bosma [3] has derived the Green's function which relates the magnetic field in the gyromagnetic medium, i.e. ferrite to the electric field

0-7803-7239-5/02/$10.00 © 2002 IEEE

anywhere in the disc. Using the same approach, the Green's function that relates the electric field to the magnetic field at each slot can be solved by referring to the positions of the slots and it was found that the Green's function matrix becomes

$$\begin{pmatrix} H_1 \\ H_2 \\ H_3 \\ H_4 \\ H_5 \\ H_6 \end{pmatrix} = \begin{bmatrix} \begin{pmatrix} \tilde{G}_1 & \tilde{G}_2 \\ \tilde{G}_2 & \tilde{G}_1 \end{pmatrix} & \begin{pmatrix} \tilde{G}_3 & \tilde{G}_4 \\ \tilde{G}_4 & \tilde{G}_3 \end{pmatrix} & \begin{pmatrix} \tilde{G}_5 & \tilde{G}_6 \\ \tilde{G}_6 & \tilde{G}_5 \end{pmatrix} \\ \begin{pmatrix} \tilde{G}_5 & \tilde{G}_6 \\ \tilde{G}_6 & \tilde{G}_5 \end{pmatrix} & \begin{pmatrix} \tilde{G}_1 & \tilde{G}_2 \\ \tilde{G}_2 & \tilde{G}_1 \end{pmatrix} & \begin{pmatrix} \tilde{G}_3 & \tilde{G}_4 \\ \tilde{G}_4 & \tilde{G}_3 \end{pmatrix} \\ \begin{pmatrix} \tilde{G}_3 & \tilde{G}_4 \\ \tilde{G}_4 & \tilde{G}_3 \end{pmatrix} & \begin{pmatrix} \tilde{G}_5 & \tilde{G}_6 \\ \tilde{G}_6 & \tilde{G}_5 \end{pmatrix} & \begin{pmatrix} \tilde{G}_1 & \tilde{G}_2 \\ \tilde{G}_2 & \tilde{G}_1 \end{pmatrix} \end{bmatrix} \begin{pmatrix} E_1 \\ E_2 \\ E_3 \\ E_4 \\ E_5 \\ E_6 \end{pmatrix} \quad (1)$$

IV. SCATTERING MATRIX

The 6×6 scattering matrix of the three-port CPW circulator is written as follows. Their derivations are not described here for brevity but can be found in [2].

$$\begin{pmatrix} b_1 \\ b_2 \\ b_3 \\ b_4 \\ b_5 \\ b_6 \end{pmatrix} = \begin{bmatrix} \begin{pmatrix} S_{11} & S_{12} \\ S_{12} & S_{11} \end{pmatrix} & \begin{pmatrix} S_{31} & S_{32} \\ S_{32} & S_{31} \end{pmatrix} & \begin{pmatrix} S_{51} & S_{52} \\ S_{52} & S_{51} \end{pmatrix} \\ \begin{pmatrix} S_{51} & S_{52} \\ S_{52} & S_{51} \end{pmatrix} & \begin{pmatrix} S_{11} & S_{12} \\ S_{12} & S_{11} \end{pmatrix} & \begin{pmatrix} S_{31} & S_{32} \\ S_{32} & S_{31} \end{pmatrix} \\ \begin{pmatrix} S_{31} & S_{32} \\ S_{32} & S_{31} \end{pmatrix} & \begin{pmatrix} S_{51} & S_{52} \\ S_{52} & S_{51} \end{pmatrix} & \begin{pmatrix} S_{11} & S_{12} \\ S_{12} & S_{11} \end{pmatrix} \end{bmatrix} \begin{pmatrix} a_1 \\ a_2 \\ a_3 \\ a_4 \\ a_5 \\ a_6 \end{pmatrix} \quad (2)$$

The inputs for CPW slots are considered in pairs, and the fields of a pair of CPW slots have the same magnitude but are 180° out of phase, thus $a_2 = -a_1$, $a_4 = -a_3$, $a_6 = -a_5$, and $b_2 = -b_1$, $b_4 = -b_3$, $b_6 = -b_5$. Therefore, the 6×6 matrix above can be simplified and expressed in the following matrix form.

$$\begin{pmatrix} b_1 \\ b_3 \\ b_5 \end{pmatrix} = \begin{bmatrix} S_A & S_B & S_C \\ S_C & S_A & S_B \\ S_B & S_C & S_A \end{bmatrix} \begin{pmatrix} a_1 \\ a_3 \\ a_5 \end{pmatrix} \quad (3)$$

where $S_A = S_{11} - S_{12}$ (4)

$S_B = S_{31} - S_{32}$ (5)

$S_C = S_{51} - S_{52}$ (6)

Note: S_A, S_B and S_C are actually the scattering parameters corresponding to the transfer functions of two input slots to one output slot. Here, S_A, S_B and S_C are known as the modified reflection, transmission and isolation coefficients.

V. SEMICONDUCTOR CIRCULATOR DESIGN EXAMPLE

N-type Indium Antimonide (InSb) with $\varepsilon_r = 17.7$ was chosen to be the material for the design of the six-slot semiconductor junction circulator. Losses in the semiconductor plasma are governed by electron collisions at an average frequency $\nu_c = 2.51 \times 10^{11}$ s^{-1} at 77K. The external magnetic flux density applied to the circulator is fixed at 0.85 Tesla. This gives the gyroelectric ratio of $\kappa/\varepsilon = 0.5535$ [4-5] at the center frequency, i.e. 60 GHz where the effective permittivity is positive. Referring to its predicted performance in Fig. 2, it can be observed that the 15dB isolation bandwidth only covers from 58GHz to 62GHz. This device has a very narrow bandwidth as the design curve only intersects the perfect circulation condition [2] at one point. Alternatively, broadband circulators can be designed using the frequency-tracking technique that will be discussed in section VIII.

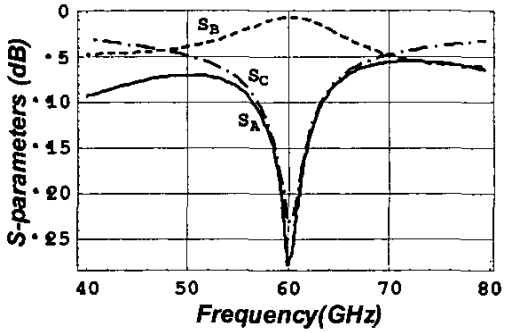

Fig. 2 Predicted performance of a six-slot n-type InSb junction circulator. R=0.49mm, ψ=0.15 rad, ε_d=17.7 and κ/ε=0.5535 at 60GHz.

VI. FERRITE CIRCULATOR DESIGN EXAMPLE

A "dual" ferrite 6-port circulator has been designed and simulated using a commercial Finite Element Modelling (FEM) i.e. Ansoft HFSS in order to provide an independent field simulation. The reasons for designing a "dual" ferrite circulator are because (a) commercial FEM solvers to date do not allow a gyroelectric material to be defined and (b) this will provide a comparison of the dualities between the six-port ferrite and semiconductor circulators.

Since a one-to-one duality between the frequency characteristics of gyroelectric and gyromagnetic circulators can be achieved by interchanging the electric and magnetic wall boundaries, microstrips were used as the interconnects to the ports in the six-port ferrite junction circulator. This is because microstrip sets up the required operating TM mode in order to couple signals into or out of the junction through the ports. The ferrite junction circulator discussed here is connected to 3 pairs of microstrips in which the signals in each pair are 180° out of phase with each other.

The ferrite is chosen to be Yttrium Iron Garnet (G-113) with a saturation magnetization $4\pi M_s$ of 1780 G. The center frequency of the circulator is chosen to be 9.18GHz as ferrite circulators cannot operate well above 40GHz due to limited saturation magnetization at about 5500 Gauss. In order to allow a direct comparison to

the six-slot CPW semiconductor circulator described in section V, the ferrite circulator is designed in the same region on the perfect circulation curves as the semiconductor circulator where its gyromagnetic ratio κ/μ is 0.5429 and its effective permeability is positive at 9.18GHz.

As shown Fig. 3, it was found that the designed ferrite circulator also has a narrow bandwidth, i.e. 15dB isolation from 8.8GHz to 9.6GHz.

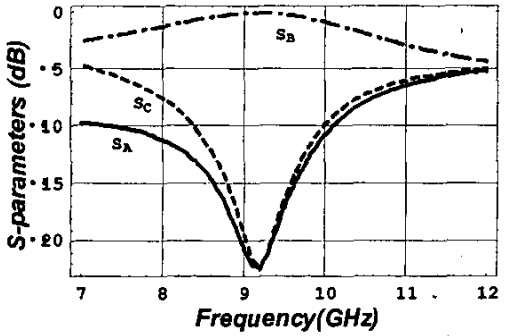

Fig. 3 Predicted frequency response of a six-port YIG junction circulator. R=3.4mm, ψ=0.17 rad, ε_d =15 and κ/ε=0.5429 at 9.18GHz.

VII. FIELD DISTRIBUTIONS

The RF electric field distribution for a three-port ferrite junction circulator has been presented by Newman and Krowne in [6]. Extending the gyromagnetic analysis to the gyroelectric case, the magnetic field at an interior response point of the semiconductor disc is expressed in terms of the incident electric field and its scattering parameters [7]. The magnetic field distribution in any point inside the six-port semiconductor disc can be expressed as:

$$H_z(r,\phi) = [(1+S_A)(\tilde{G}_1 - \tilde{G}_2) + S_B(\tilde{G}_3 - \tilde{G}_4) + S_C(\tilde{G}_5 - \tilde{G}_6)]E_{incident} \quad (7)$$

The RF magnetic field distribution of the six-slot semiconductor disc at three frequencies, i.e. below, above and at the center frequency are computed for the first time (using Mathematica) and compared with the electric field distributions for the ferrite disc obtained from the Ansoft HFSS simulation.

From the contour plots, it can be observed that the patterns of the plots are frequency dependent. Below the center frequency, it can be observed that the lightly colored regions which represent weaker fields are not aligned in both semiconductor (Fig. 4(a)) and ferrite (Fig. 4(b)) circulators. At the center frequencies, the field patterns in both circulators matches the field pattern of a resonator of TE_{110} mode. In Fig. 4(c), the darker regions are more concentrated on both the right and left sides of the disc, which means that the CPW input signals for the semiconductor disc at ports 1 and 2 are transmitted to ports 3 and 4. A similar situation can also be observed in the ferrite circulator as shown in Fig. 4(d) such that there is a light colored vertical strip located in the middle of the disc and ports 5 and 6 are isolated. Stronger fields are concentrated at the two sides of the ferrite disc. Above the center frequency, the field patterns in both circulators start to break up as the weaker field regions start to spread to a wider area in the disc. This similar result has also been observed in conventional three-port ferrite [6] and semiconductor [7] circulators.

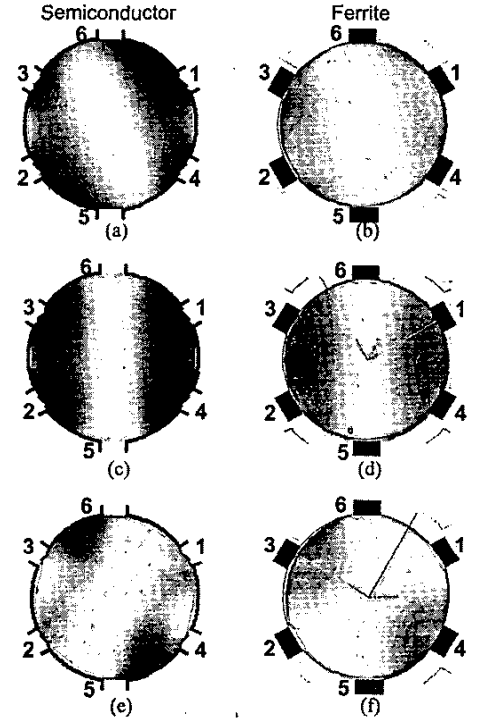

Fig. 4. Magnetic field distributions for n-type InSb junction circulator (computed from Mathematica) (a) 50GHz, (c) 60GHz and (e) 70GHz. Electric field distribution for YIG junction circulator (modelled using Ansoft HFSS) (b) 8GHz, (d) 9.18GHz and (f) 10GHz. Strong fields are represented by darker color. Ports 1 and 2 are input ports while ports 5 and 6 are isolated.

VIII. BROADBAND SEMICONDUCTOR CIRCULATOR DESIGN EXAMPLE

Wu and Rosenbaum [8] showed that a broadband ferrite circulator can be designed by tracking between the perfect circulations and the calculated variations with gyromagnetic ratio κ/μ where the effective permeability μ_{eff} is positive. Special attention is required for ferrite circulator designed below the resonance frequency where $\mu_{eff}<0$ due to low field losses [9].

In a semiconductor circulator, such problem is not encountered. Therefore, a broadband circulator can be designed by extending circulation solutions for both $\varepsilon_{eff} > 0$ and $\varepsilon_{eff} < 0$. Careful choice of the surrounding dielectric medium, the radius and the coupling angle of the disc gives the tracking behavior of this six-slot device shown in Fig. 5(a) and (b). It can be seen that both $k_{eff}R$ and Z_d/Z_{eff} (shown as dashed lines) closely follow the perfect circulation curves. As a result, a broadband 60 GHz six-slot semiconductor circulator is designed and Fig. 6 shows predicted 15dB isolation performance from 40 GHz to 70GHz.

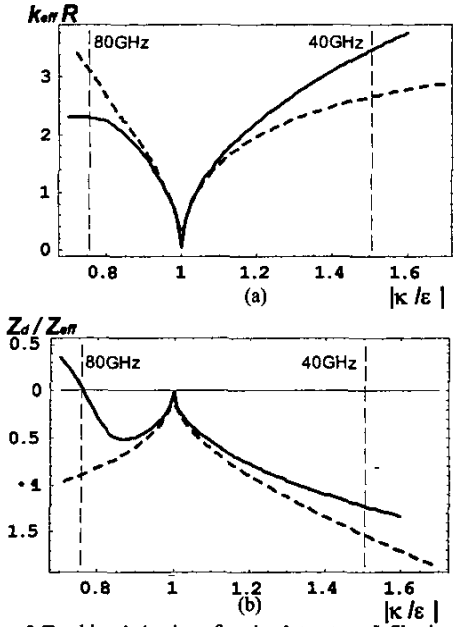

Fig. 5 Tracking behavior of a six-slot n-type InSb circulator with (a) first and (b) second circulation conditions. Design curves are shown as dashed lines while solid lines represent the perfect circulation curves of ψ=0.15 rad.

IX. CONCLUSIONS

The magnetic field distributions of the six-slot semiconductor junction circulator have been calculated for the first time and compared with the electric field distribution of the six-port microstrip ferrite junction circulator using a commercial software. Both circulators have narrow bandwidth and they are designed for the frequency region where $\varepsilon_{eff}>0$ and $\mu_{eff}>0$ respectively. From their magnetic and electric field contour plots, it can be observed that the field patterns for both circulators are very similar including misalignment of null patch below center frequency, field distribution which resembles TE_{110} field pattern at center frequency and field distortions at higher frequencies.

The curve tracking technique is also demonstrated theoretically between the perfect circulation curves and the design curve to obtain broadband six-slot semiconductor junction circulator. A broadband circulator centered at 60 GHz has been designed to operate in the frequency regions where its $\varepsilon_{eff}<0$ and $\varepsilon_{eff}>0$. Our next objective is to fabricate such a device and experimentally measure its performance. Lastly, since this device is supported by CPW feeder lines, this might lead to a integration of such circulators into MMICs.

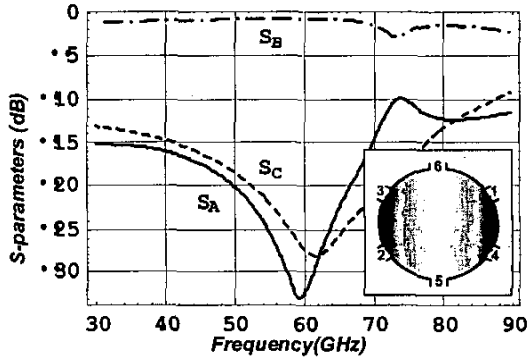

Fig. 6 Predicted performance of n-type InSb junction circulator. R=0.65mm, ψ=0.14 rad, ε_d =10.2, B_0=0.43T and κ/ε =1.0064 at 60GHz. The inset shows the magnetic field distribution at 60GHz. As $\varepsilon_{eff}<0$, the fields do not penetrate throughout the disc and are concentrated at the sides of the disc.

REFERENCE

[1] C. K. Yong, R. Sloan and L.E. Davis, "A Ka-Band Indium Antimonide Junction Circulator," *IEEE Trans. Microwave Theory Tech.*, Vol. MTT-49, No.6, pp. 1101-1106, June 2001.

[2] Zee M. Ng, Lionel. E. Davis and Robin Sloan, "Coplanar Waveguide (CPW) Gyroelectric Circulator", Accepted for publication in *Journal of RF and Microwave Computer-Aided Engineering*

[3] H. Bosma, "On Stripline Y-circulation at UHF," *IEEE Trans. Microwave Theory Tech.*, Vol. MTT-12, pp 61-72, Jan. 1964.

[4] L.E. Davis and R. Sloan, "Predicted Performance of Semiconductor Junction Circulators with Losses," *IEEE Trans Microwave Theory Tech.*, vol. MTT-41, No. 12, pp.2243-2247, Dec. 1993.

[5] R. Sloan, C. K. Yong and L. E. Davis, "Broadband Theoretical Gyroelectric Junction Circulator Tracking Behavior at 77K," *IEEE Trans. Microwave Theory Tech.*, Vol. MTT-44, No. 12, pp. 2655-2659, Dec. 1996.

[6] H. S. Newman and C. M. Krowne, " Analysis of Ferrite Circulator by 2-D Finite-Element and Recursive Green's Function Techniques," *IEEE Trans. Microwave Theory Tech.*, vol. MTT-46, No.2, pp. 167-177, Feb.1998.

[7] Z. M. Ng, R. Sloan and L.E. Davis, "Field Distribution in a Semiconductor Junction Circulator," *Electronics Letters*, Vol. 36, No. 12, 8th Jun. 2000, pp.1034-1035.

[8] Y. S. Wu and F. J. Rosenbaum, "Wide-band Operation of Microstrip Circulators," *IEEE Trans. Microwave Theory Tech.*, Vol. MTT-22, pp. 849-856, Oct. 1974.

[9] E. Schloemann and R. E. Blight, "Broad-band Stripline Circulators based on YIG and Li-Ferrite Single Crystal," *IEEE Trans. Microwave Theory Tech.*, Vol. MTT-34, pp. 1394-1400, Dec. 1986.